

Note

On a Numerical Method for Quasi-conformal Grid Generation

1. INTRODUCTION

In this note we generate some quasi-conformal grids by using fast Fourier transforms and path integrals. Thus this method is rapid as opposed to other elliptic methods. In particular we generate such grids around airfoils. The method uses potential flow equations of fluid flow in the construction of these grids. We briefly discuss about embedding this method within a general framework. The main purpose of this note is to discuss this specific but fast method and generate the grids which may have practical applications. This note is not meant to be an exhaustive treatment on quasi-conformal grid generation and thus we do not discuss their applications here.

2. PRELIMINARIES ON COMPRESSIBLE FLOW

Here we briefly discuss the compressible flow equations which are pertinent to our grid generation. The reader is referred to [1, 2] for details.

Let Ω_z be the domain exterior to a closed body. In particular we will consider the closed body to be an airfoil. The potential flow equations of compressible fluid are given by [1, 2]

$$\nabla \cdot (\rho \mathbf{q}) = 0; \quad \nabla \times \mathbf{q} = 0; \quad p = \rho^\gamma, \quad (2.1)$$

where the variables have their usual meaning. Introduce the potential and the stream functions ϕ and ψ respectively through

$$\rho \mathbf{q} = \nabla \times (c\psi \mathbf{k}); \quad \mathbf{q} = \nabla \phi. \quad (2.2)$$

Here c is an arbitrary constant. These equations in the potential plane $w = \phi + i\psi$ are then given by [1, 2]

$$\theta_\phi - K^{-1}v_\psi = 0, \quad \theta_\psi + Kv_\phi = 0. \quad (2.3)$$

Above and below ϕ , ψ , θ , v respectively denote potential, stream function, flow

direction and the Prandtl Meyer function. The functions K and v in (2.3) are defined as

$$K = c \frac{\beta}{\rho(q(M))}; \quad v = \int_1^q \frac{\beta dq}{q}. \quad (2.4), (2.5)$$

We use the notation $\beta^2 = 1 - M^2$. The density " ρ " is related to Mach number " M " and speed " q " through the Bernoulli's law and the pressure-density relation for an ideal gas. The domain Ω_z maps into Ω_w , where Ω_w is the exterior of a slit, the slit ∂w being the image of the body ∂z . The mapping $z(w): \Omega_z \rightarrow \Omega_w$ is given by

$$\begin{aligned} dz &= \frac{e^{i\theta}}{q} \left(d\phi + i \frac{c}{\rho} d\psi \right) \\ &= \frac{e^{i\theta}}{2q} \left\{ \left(1 + \frac{c}{\rho} \right) d\omega + \left(1 - \frac{c}{\rho} \right) d\bar{\omega} \right\}. \end{aligned} \quad (2.6)$$

Notice that this mapping is not conformal. If the following variables are introduced

$$\tau = -v + i\theta; \quad \mu = \frac{1-K}{1+K}, \quad (2.7), (2.8)$$

then the equations (2.3) can be written in compact form as [2]

$$\tau_{\bar{\omega}} = \mu \tau_{\omega}. \quad (2.9)$$

Equations (2.6) and (2.9) together define the flow in the z -plane. Now introduce a conformal mapping $w_{\bar{\sigma}} = 0$, mapping the w -plane into the interior of a unit circle $|\sigma| < 1$ so that (2.9) and (2.6) respectively reduce to

$$\tau_{\bar{\sigma}} = \chi \tau_{\sigma} \quad (2.10)$$

and

$$dz = \frac{e^{i\theta}}{2q} \left\{ \left(1 + \frac{c}{\rho} \right) \omega_{\sigma} d\sigma + \left(1 - \frac{c}{\rho} \right) \bar{\omega}_{\bar{\sigma}} d\bar{\sigma} \right\}, \quad (2.11)$$

where

$$\chi = \frac{\mu(\bar{\omega}_{\sigma})}{\omega_{\sigma}}. \quad (2.12)$$

From mapping (2.11) we have

$$z_{\sigma} = \frac{e^{i\theta}}{q} \left(1 + \frac{c}{\rho} \right) \omega_{\sigma}; \quad z_{\bar{\sigma}} = \frac{e^{i\theta}}{q} \left(1 - \frac{c}{\rho} \right) (\bar{\omega}_{\sigma}). \quad (2.13), (2.14)$$

For the purpose of exposition, it is preferable to write Eqs. (2.13) and (2.14) as

$$z_{\bar{\sigma}} = f(\tau(\sigma), \sigma); \quad z_{\sigma} = g(\tau(\sigma), \sigma), \quad (2.15), (2.16)$$

where the functions f and g are easily identified from (2.13) and (2.14). Notice that both are explicit functions of τ (also $\bar{\tau}$) and σ .

We note that the function χ in Eq. (2.10) depends on K through (2.12) and (2.8). One notices from (2.4) that K depends on the choice of the pressure-density relation and the constant "c." Now if the $p - \rho$ relation in Eq. (2.1) is modified to be $(p - 1) = \gamma(1 - 1/\rho)$, then it can be shown that [3, 5]

$$\rho = \beta/\beta_{\infty}. \quad (2.17)$$

The constant "c" is chosen to be $1/\beta_{\infty}$, so that Eq. (2.17) reduces to

$$\rho/c = \beta. \quad (2.18)$$

In this approximation, the constant K , given by Eq. (2.4) equals one. It is seen from (2.8) and (2.12) that with $K = 1$, $\chi = 0$ and Eq. (2.10) reduces to

$$\tau_{\bar{\sigma}} = 0. \quad (2.19)$$

This approximation is known as tangent gas approximation. In this approximation, computation of τ is somewhat straightforward. The theory developed here will be useful in the following section.

3. GRID GENERATION

We consider the problem of grid generation as mapping of the interior of a unit circle in σ -plane onto the exterior of a closed body in the z -plane such that the unit circle maps onto the body. A quasi-conformal mapping can be generated by solving

$$z_{\bar{\sigma}} = h(\sigma), \quad (3.1)$$

where $h(\sigma)$ is an arbitrary function. It is known that if $h(\sigma)$ is Hölder continuous, then $z_{\sigma}(\sigma)$ and $z(\sigma)$ are given by [6]

$$z(\sigma) = -\frac{1}{\pi} \iint_{S_{\Omega}} \frac{h(\zeta)}{\zeta - \sigma} d\xi d\eta, \quad (3.2)$$

$$z_{\sigma} = -\frac{1}{\pi} \iint_{S_{\Omega}} \frac{h(\zeta) - h(\sigma)}{(\zeta - \sigma)^2} d\xi d\eta. \quad (3.3)$$

Integration over the entire domain can be performed using (3.2) to generate the grids. However, by using this method, determining the image of each lattice point of the circle plane requires the evaluation of one double integral. This is a rather

tedious and numerically expensive task. In order to make this method numerically viable, consider pinning the arbitrary function $h(\sigma)$ in (3.1) to be $f(\tau(\sigma), \sigma)$ given by (2.13)–(2.16), i.e.,

$$z_{\bar{\sigma}} = f(\tau(\sigma), \sigma); \quad (3.4)$$

then (3.2) and (3.3) become (see Eqs. (2.15) and (2.16))

$$z_{\sigma} = g(\tau(\sigma), \sigma), \quad z(\sigma) = \int g(\tau(\sigma), \sigma) d\sigma + \int f(\tau(\sigma), \sigma) d\bar{\sigma}, \quad (3.5), (3.6)$$

subject to the constraint that τ satisfies

$$\tau_{\bar{\sigma}} = \chi\tau_{\sigma}. \quad (3.7)$$

In fictitious gas (tangent gas) approximation this constraint reduces to

$$\tau_{\bar{\sigma}} = 0. \quad (3.8)$$

It is obvious that generating the grids by using the path-integral (3.6) will require a considerably smaller number of operations than by using the double integral formulation (3.2). This is, however, true only if evaluation of τ does not involve a considerable number of operations. Undoubtedly this requires the computation of τ by using Eq. (3.8), rather than Eq. (3.7). Thus our specific fast algorithm consists of the following steps:

(i) Compute the function $\tau(\sigma)$ using the fast Fourier transforms. For details on this see [3]. Briefly, this stage consists of expressing τ as a Taylor series and then evaluating τ on the unit circle $\sigma = 1$ at a specified free stream Mach number and angle of attack. Use of FFT is made in this computation. This computation requires $N \log N$ operations with N grid points on the unit circle. Once τ ($\sigma = 1$) is known, τ at the interior grid points are evaluated using the Taylor series. Considerable computational savings are favored when use is made of FFT in this evaluation [2]. With N number of grid points also in the radial direction, the total number of operations is $N^2 \log N$. These operations provide the value of τ at all (N^2) interior points.

(ii) Evaluate the functions $f(\tau(\sigma), \sigma)$ and $g(\tau(\sigma), \sigma)$ by using the explicit relations (2.13)–(2.16).

(iii) Generate the grids by evaluating the path integrals using (3.6).

We point out that the hidden parameters that can be tuned to generate different types of grids are Mach number " M_{∞} " and angle of attack $\theta_{\infty} = \alpha$." This fact has been mentioned in step (i) above. For our purpose of grid generation here, M_{∞} and α should be thought of as flexible parameters.

We end this section by analysing the ratio $|\lambda(\sigma)| = |z_{\bar{\sigma}}/z_{\sigma}|$ which plays an important role in the mapping $f(\sigma): \Omega_{\sigma} \rightarrow \Omega_z$. From (2.13) and (2.14) we have

$$|\lambda(\sigma)| = \left| \frac{z_{\bar{\sigma}}}{z_{\sigma}} \right| = \left| \frac{1 - c/\rho}{1 + c/\rho} \right|. \quad (3.9)$$

For our approximation (2.18), (3.9) reduces to

$$|\lambda(\sigma)| = \left| \frac{\beta - 1}{\beta + 1} \right| = \left| \frac{\sqrt{1 - M^2} - 1}{\sqrt{1 - M^2} + 1} \right|. \quad (3.10)$$

The Jacobian of this quasi-conformal mapping [5] is given by

$$J = |z_\sigma|^2 - |\bar{z}_\sigma|^2 = (1 - |\lambda|^2) |z_\sigma|^2. \quad (3.11)$$

Note from (3.10) and (3.11) that for $M=0$, we have $\lambda=0$ and $J=|z_\sigma|^2$. This corresponds to conformal mapping. However, we should notice that $M=1$ corresponds to $|\lambda|=1$ which implies $J=0$ and hence the entire Ω maps into a line $y=g(x)$. This line depends on the form of $z(\sigma)$. These remarks will be useful in discussing the numerical results in the next section.

4. NUMERICAL RESULTS AND DISCUSSIONS

We apply our algorithm to generate quasi-conformal grids around NACA0012 airfoil. We have taken uniformly spaced grid points in the radial and angular directions in the circle plane. In all our runs, the number of grid points in angular and radial directions have been taken to be 129 and 21, respectively. Thus we have a fixed set of grid points in the circle plane. We fix $\alpha=0$ in order to generate symmetric grids around the airfoil. This leaves the " M_∞ " as a free parameter. On mapping the grids of the circle plane onto the exterior of the airfoil, we generate the grids that one is usually interested in. The properties of these grids will vary as the M_∞ is changed. We show these grids for various values of M_∞ .

In Figs. 1, 2, 3, and 4 we show the grids generated for $M_\infty=0$, $M_\infty=0.5$, $M_\infty=0.6$, and $M_\infty=0.8$, respectively. By visual inspection of these figures, we note that the grids are orthogonal in Fig. 1, which corresponds to conformal mapping ($M=0$, $\lambda=0$, see Eq. (3.10)). For $M \neq 0$, we see in Figs. 2, 3, and 4 that the grids are not orthogonal. We especially notice the following which is consistent with the theory:

(i) The deviation from orthogonality increases as the parameter " M_∞ " increases. This can be noticed by comparing any particular cell in these figures. Consider visually comparing the cells marked "I" in these figures which are images of the same grid cell of the circle plane.

(ii) With parameter " M " increasing, the length (h) of one side of each grid cell keeps increasing, while the other side (w) keeps decreasing. If we refer to this ratio h/w as cell aspect ratio and denote it by " A ," then we have $dA/dM > 0$ for each grid cell. It is expected that as " M_∞ " approaches one " w " approaches zero; thereby all grid cells collapse onto a line. This is in agreement with the fact that the Jacobian $J=0$ for $M=1$. However, $M=1$ is a case of parabolic degeneracy (see Eq. (2.3)) and there are technical problems in this singular limit. In any case for the

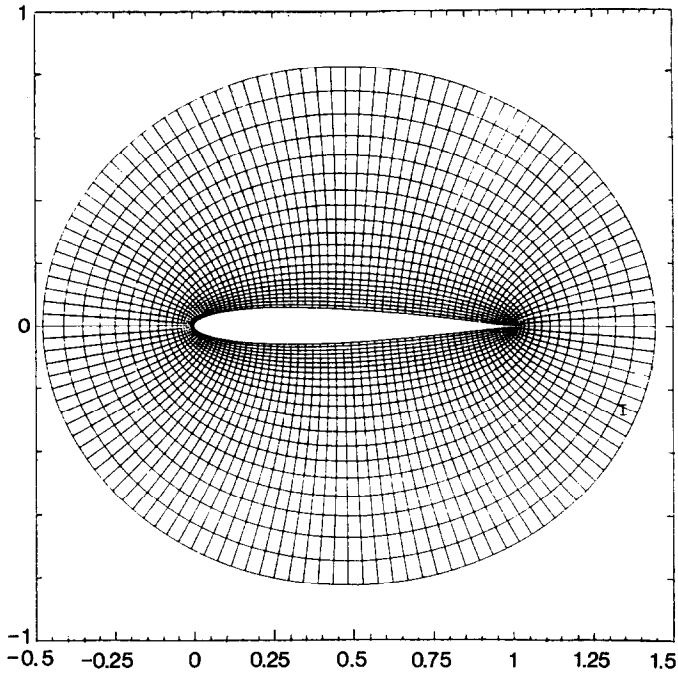


FIGURE 1

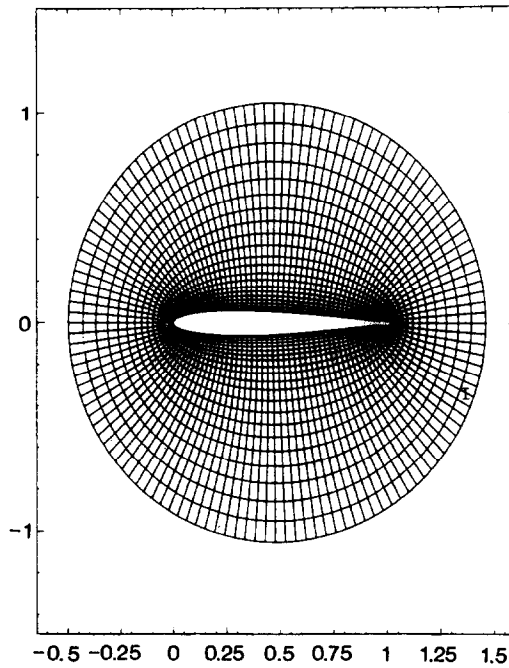


FIGURE 2

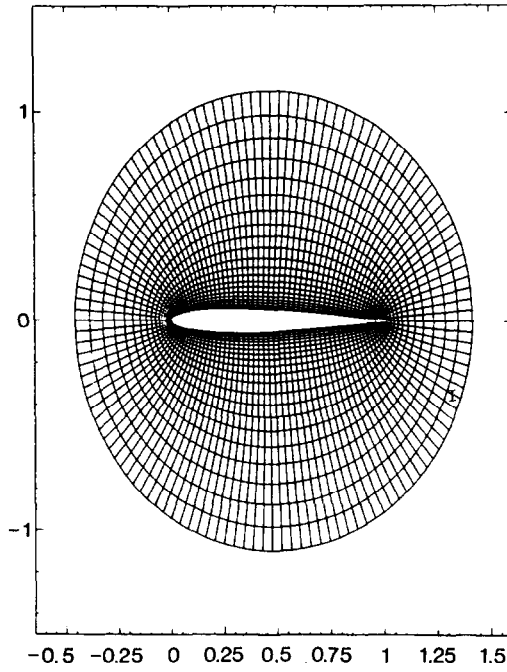


FIGURE 3

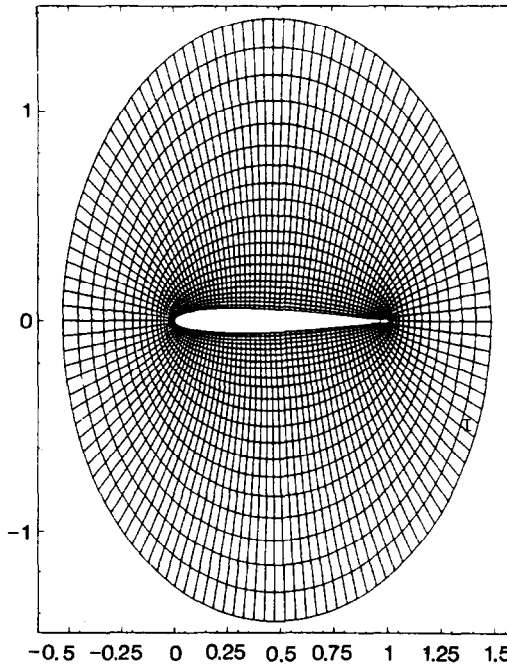


FIGURE 4

purpose of grid generation, such degenerate situations are pathological and are of no use.

So, here we have a method which allows one to generate grids whose properties can be changed by varying the parameter M_∞ . These grids may be useful in problems where the field variable changes more rapidly in one direction than the other direction. Such grids have been previously used by the author in solving Euler equations using finite volume method using flow 52s code [3]. Similarly we can generate grids by varying the other free parameter α . However such grids for $\alpha \neq 0$ will be severely curved and unsymmetric and seem to be of not much interest.

The above two free parameters enter into our formulation through auxillary equations whose unique solution requires the specification of these parameters. Here we have used the compressible fluid flow equations as auxillary equations. Here application is somewhat limited due to lack of more adjustable parameters. The possibility of the existence of other sets of auxillary equations which will serve the purpose equally well or even better is not ruled out. It must be emphasized that a more general method would be to use Eq. (3.2) to generate the grids. This will allow one to incorporate as many parameters as one wishes in the choice of the function $h(\sigma)$ in (3.2). Thus a wide variety of two-dimensional quasi-conformal grids can be generated by adjusting these parameters. But this is at present numerically expensive due to the area integral in Eq. (3.2). Only a fast method for evaluating this double integral will make this method numerically favorable, beside being very general in application. Some work along this direction is reported in [4] and more exhaustive treatment on this issue will be reported elsewhere.

It is a pleasure to thank Lawrence Sirovich for comments and discussions. This research in part has been supported by the NSF Grant DMS-8803669 to Texas A&M University and by the DARPA Grant N00014-86-K0754 to Brown University.

REFERENCES

1. L. BERS, *Mathematical Aspects of Subsonic and Transonic Gas Dynamics* (Wiley, New York, 1958), p. 164.
2. P. DARIPA, *J. Comput. Phys.* **88**, 337 (1990).
3. P. DARIPA AND L. SIROVICH, *J. Comput. Phys.* **63**, 311 (1986).
4. P. DARIPA, IMA Preprint No. 592.
5. L. C. WOODS, *The Theory of Subsonic Plane Flow* (Cambridge Univ. Press, London/New York, 1961).
6. R. COURANT AND D. HILBERT, *Methods of Mathematical Physics, Vol. II* (Wiley Interscience, New York, 1961), p. 830.

RECEIVED: September 6, 1989; REVISED: April 2, 1990

PRABIR DARIPA
Division of Applied Mathematics,
Department of Mathematics,
Texas A&M University, College Station, Texas 77843